

THERMODYNAMIC STABILITY OF RECODING RNA PSEUDOKNOTS AND
RIBOSOMAL FRAMESHIFTING

A Senior Honors Thesis

by

BRIAN RAY CANNON

Submitted to the Office of Honors Programs
& Academic Scholarships
Texas A&M University
in partial fulfillment for the designation of

UNIVERSITY UNDERGRADUATE
RESEARCH FELLOW

April 2001

Group: Biochemistry

THERMODYNAMIC STABILITY OF RECODING RNA PSEUDOKNOTS AND
RIBOSOMAL FRAMESHIFTING

A Senior Honors Thesis

by

BRIAN RAY CANNON

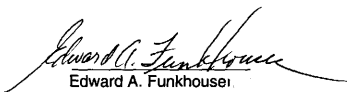
Submitted to the Office of Honors Programs
& Academic Scholarships
Texas A&M University
in partial fulfillment of the requirements of the

UNIVERSITY UNDERGRADUATE
RESEARCH FELLOWS

Approved as to style and content by:



David P. Giedroc
(Fellows Advisor)



Edward A. Funkhouser
(Executive Director)

April 2001

Group: Biochemistry

ABSTRACT

Programmed ribosomal frameshifting is a method of regulation of protein expression in which a change in reading frame during translation brings about the formation of an alternative gene product. This process is an important part of the replicative machinery of many RNA viruses, including HIV-1, the causative agent of AIDS. Programmed -1 frameshifting is commonly stimulated via an as yet undetermined mechanism that requires an RNA structural motif in the mRNA coding sequence known as an RNA pseudoknot, found just downstream of the site of -1 slippage. Recently, it was shown that engineering two structural features of the pseudoknots derived from tobacco yellow mosaic virus (a specifically placed loop 2 adenosine), TYMV, and mouse mammary tumor virus (an unpaired adenosine at the stem 1 – stem 2 junction), MMTV could restore efficient frameshifting to a functionally inactive pseudoknot. Thermodynamic analysis presented here shows that a mutant pseudoknot lacking the loop 2 adenosine forms a pseudoknot structure which is stabilized by 1.4 ± 0.5 kcal mol⁻¹. In contrast, two other pseudoknots, in which the junction adenosine residue was substituted with guanosine and the other one in which the loop 2 adenosine was replaced with guanosine, both formed moderately less stable structures. All three RNAs display frameshifting efficiencies greatly reduced relative to the wild type RNA. Although these findings suggest that there is no clear correlation between pseudoknot stability and frameshifting efficiency, our data does suggest that a specific interaction between a loop 2

adenosine and helical stem 1 makes a measurable contribution to pseudoknot stability.

ACKNOWLEDGEMENTS

I would like to thank my advisor, Dr. David P. Giedroc for allowing me to work in his laboratory for the past four years, and for his instruction and patience with me throughout the course of this project. Working with him has opened me up to numerous scientific opportunities, among which will include attending graduate school at the Johns Hopkins University Program in Molecular Biophysics next fall.

I must also offer up special thanks to the graduate students who helped me the most closely throughout the course of this project: Paul L. Nixon and Dr. Carla A. Theimer. I have also valued the fellowship and encouragement of my other colleagues (and friends) in lab: Julius Apuy, Laura Busenlehner, Xiaohua Chen, Mario Pennella, Jody Smith, Endah Sulistiju, Saritha Suram, Mike Van Zile, and Lyndsay Windham.

Additionally, I would like to thank my parents Steve and Diane Cannon for funding my education at Texas A&M, and for their ongoing guidance and support of my educational endeavors.

In the spirit of 1 Corinthians 10:31, I would like to dedicate this project to the glory of God. Since becoming a Christian shortly after my freshman year, He has continually blessed and encouraged me through the work that He has given me to do relating to this project. I thank God for the strength and peace that He has provided throughout all struggles in lab. I would have quit science long ago had it not been for His guidance and love. I give turn to him any credit

that might be directed towards myself, and recognize Him as the source of any good that has or will come out of my feeble life. "For I have been crucified with Christ; and it is no longer I who live, but Christ who lives in me. The life which I now live in the flesh I live by faith in the Son of God, who loved me and gave himself up for me" (Galatians 2:20).

TABLE OF CONTENTS

	Page
ABSTRACT.....	iii
ACKNOWLEDGEMENTS.....	v
TABLE OF CONTENTS.....	vii
LIST OF FIGURES.....	viii
LIST OF TABLES.....	ix
 CHAPTER	
I INTRODUCTION.....	1
II RESULTS.....	8
Analysis of Thermal Denaturation Melting Profiles.....	8
Thermodynamic Analysis of IBV-RNAs.....	11
ΔG_{tot} vs. Frameshifting Efficiency.....	15
III CONCLUSIONS.....	18
IV MATERIALS AND METHODS.....	20
RNA Purification.....	20
UV Thermal Denaturation.....	20
Differential Scanning Calorimetry Denaturation.....	21
REFERENCES.....	22
VITA.....	24

LIST OF FIGURES

FIGURE

1	Formation of an RNA Pseudoknot.....	2
2	-1 Ribosomal Frameshifting.....	3
3	Secondary Structure of WT and Mutant Pseudoknots.....	6
4	UV and DSC Melts.....	9
5	Pseudoknot Unfolding Pathway for IBV-MMTV Chimeric RNAs.....	10
6	Plot of Frameshifting Efficiency vs. $\Delta\Delta G_{1-3}^{37}$	17

LIST OF TABLES**TABLE**

1	Thermodynamic Parameters Derived From DSC Melting Profiles.....	12
2	Thermodynamic Parameters Data Derived From UV Melting Profiles.....	13

CHAPTER 1

INTRODUCTION

RNA pseudoknots are structural elements, found in all types of RNAs, including mRNA. They form as a direct result of the ability of RNA to form intramolecular Watson-Crick base pairs. A pseudoknot is a folding topology which forms when nucleotides in the loop region of an RNA hairpin form additional base pairs with some other complementary region of RNA outside of the hairpin to form a structure consisting of two stems, denoted S1 and S2, and two loop regions, denoted L1 and L2 (Figure 1). This simple fold is important in that it has been shown to be a structural component of many naturally occurring RNAs, including ribosomal RNAs, messenger RNAs, catalytic and self-splicing RNAs, and viral genomic RNAs (for a review, see Giedroc *et al.*, 2000). Furthermore, this structure plays an essential role in the viral life cycle by helping to regulate -1 ribosomal frameshifting (for a review, see Farabaugh, 1993).

In RNA viruses, programmed -1 ribosomal frameshifting is used as a method for the regulation of protein expression. The change in reading frame brought about by frameshifting allows a normally in-frame stop codon to be bypassed so that a new poly-protein fused gene product can be formed (Figure 1). By employing this regulatory system, viruses are able to code for multiple gene products with the requirement of only one ribosomal initiation event. A -1 frameshifting event has been observed between overlapping *gag* and *pro* genes

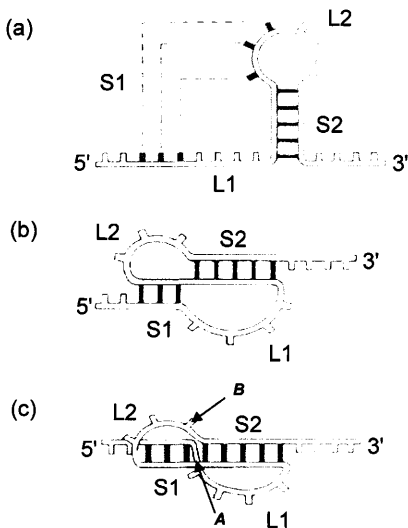
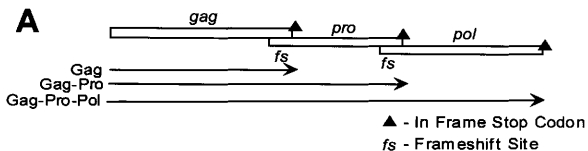


Figure 1. Formation of an RNA pseudoknot (Pleij, 1994). (a) Nucleotides in the loop 2 (L2) of an RNA hairpin region fold back and form complementary base pairs with nucleotides in another region of the RNA. (b) Base pairing forms a region consisting of two stem (S1 and S2) and two loop (L1 and L2) regions. (c) Stacking of the two stems to form a quasi-continuous RNA helix of S1 + S2 base pairs. The A arrow marks the point in the continuous strand where an intercalated nucleotide is sometimes found. The B arrow marks the 3' nucleotide in L2 closest to the helical junction.



B -1 Frameshift

No Frameshift

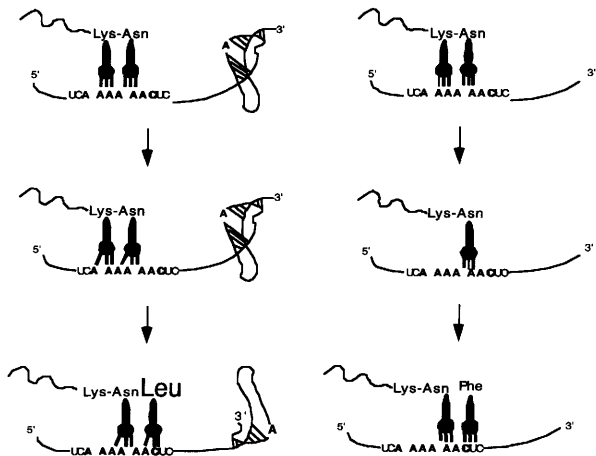


Figure 2. (a) Formation of fused gene products via -1 ribosomal frameshifting. (b) Model for -1 ribosomal frameshifting (Giedroc et al., 2000).

(Figure 2), the efficiency of which dictates the relative molar amounts of structural (gag) to replicative (pro) gene products needed for viral reproduction and infectivity (Brierly *et al.*, 1989).

Two features have been shown to be essential for frameshifting – a heptanuclear “slippery sequence” (the site where the actual frameshifting event takes place) and a downstream stimulatory structure, which commonly takes on the form of an RNA pseudoknot (Figure 1). It is known that when the ribosome encounters the pseudoknot, it pauses, possibly because the pseudoknot provides some block to ribosome movement. Either the slippery sequence or the pseudoknot by itself is insufficient to promote efficient frameshifting. Recent studies are consistent with the idea that specific structural or stability characteristics of the pseudoknot may be important in promoting the frameshifting process. One such study displays a correlation between stem 1 length and efficient -1 ribosomal frameshifting for a series of IBV-derived pseudoknots (Naphthine *et al.*, 1999). For this class of pseudoknots, it was shown that a stem 1 region consisting of 11 base pairs was optimally required for promotion of efficient frameshifting *in vitro*.

An elongated stem 1 region, however, is not an absolute structural requirement for efficient frameshifting. Examples of two pseudoknots that have seemingly bypassed the stem 1 requirement are the pseudoknot from mouse mammary tumor virus (MMTV) (Shen & Tinoco, 1995), and beet western yellows virus (BWYV) (Su *et al.*, 1999), both of which have stem 1 regions containing only 5 base pairs. Subsequent studies have shown that incorporating

structural features from the MMTV pseudoknot into a non-functional IBV pseudoknot with a short stem 1 region could restore the ability of the pseudoknot to promote efficient frameshifting (Liphardt *et al.*, 1999).

A specific feature of the MMTV pseudoknot is the presence of an intercalated adenosine residue at the stem 1 – stem 2 junction, which imparts an overall bent conformation to the molecule (Shen & Tinoco, 1995) (see Figure 1, arrow A). The insertion of this intercalated adenosine into the stem 1 – stem 2 junction of a non-functional pseudoknot with a six base pair stem 1 region was, however, insufficient to promote efficient frameshifting (Liphardt *et al.*, 1999). A second structural change was required, one in which an adenosine at the 3' position of loop 2 will form specific hydrogen bonds with the minor groove side of the helical stem 1 of the pseudoknot (see Figure 2, arrow B). Such hydrogen bonding interactions have been documented to occur in the TYMV pseudoknot (Kolk *et al.*, 1998). Changing the most 3' nucleotide of loop 2 to an adenosine residue is hypothesized to impart some additional structural or stability determinant which restores efficient frameshifting to a pseudoknot already containing an intercalated adenosine at the helical junction. This optimized structure (see Figure 3), denoted wild-type (WT) or IBV-MMTV in these studies, yielded a frameshifting efficiency of ~31% (Liphardt *et al.*, 1999). Within this structural context, the removal or substitution of the intercalated adenosine resulted in a significant reduction in frameshifting activity, reducing frameshifting efficiency to between 8%-13%. Disruption of the loop 2 adenosine resulted in a similar drop in frameshifting efficiency, to 5%-9% (Liphardt *et al.*, 1999).

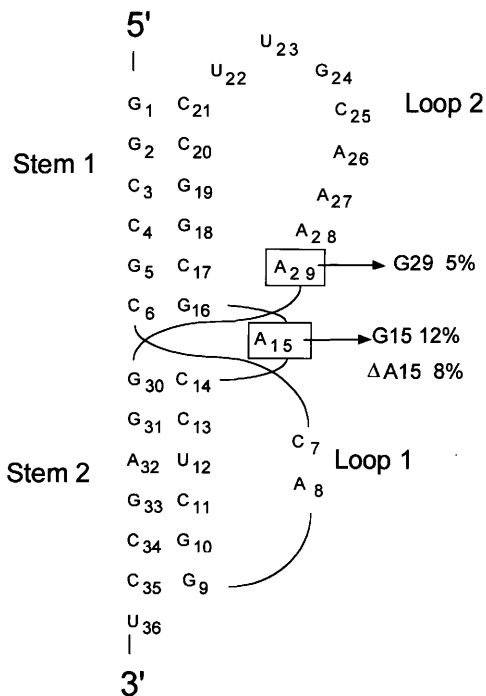


Figure 3. Secondary structure of WT-IBV pseudoknot (from Liphardt *et al.*, 1999), with mutations noted.

These functional frameshifting studies reveal that these two structural determinants make an important contribution to the ability of a pseudoknot to promote efficient frameshifting. One explanation of these functional data is that the wild-type construct provides for a very stable structure, which could provide a strong block to ribosomal movement (Figure 2), while deletion or substitution of these key structural elements would be strongly destabilizing. It is this hypothesis that the studies outlined in this thesis were designed to test. Specifically, we report here the thermodynamics of unfolding of the wild-type and three mutant IBV-MMTV chimeric pseudoknots shown in Figure 3 in order to more fully define the relationship between the thermodynamic stability of each structure and frameshifting activity. It is hoped that understanding the free energy pertaining to the stability of these interactions will facilitate a greater understanding of how these structures stimulate -1 frameshifting.

CHAPTER 2

RESULTS

Analysis of Thermal Denaturation Melting Profiles

To investigate the stabilities of the pseudoknots described in Figure 1, large-scale transcription reactions were prepared for each RNA. Melting profiles were then obtained using two thermal denaturation techniques – differential scanning calorimetry (DSC) and optically monitored thermal denaturation. All melting experiments were performed under the same buffer conditions – 10 mM 3-(N-Morpholino) propanesulfonic acid (MOPS), 50 mM KCl, pH 7.0. Experimental melting profiles were fit to an unfolding model characterized by four sequential two-state unfolding transitions. Representative melts are shown in Figure 4.

It was found that fitting the melting profiles of WT, $\Delta A15$, and G29 RNA to three transitions resulted in a ΔH_{tot} smaller than would be predicted for the unfolding of secondary structure alone ($\Delta H_{\text{predicted}} = 132 \text{ kcal mol}^{-1}$, as calculated from Xia *et al.*, 1998, data not shown); however, such a fit is physically unreasonable. Fitting to four unfolding transitions accounted for this missing enthalpy. The two large peaks in the melting profile correspond to unfolding of the two helical stems of the pseudoknot, with stem 2 unfolding first, followed by stem 1 (Figure 5). The first low temperature, low amplitude transition, which typically occurs below $t_m = 40^\circ\text{C}$, may relate to the collapse of some tertiary structure in the pseudoknot, defined here as specific interactions between the

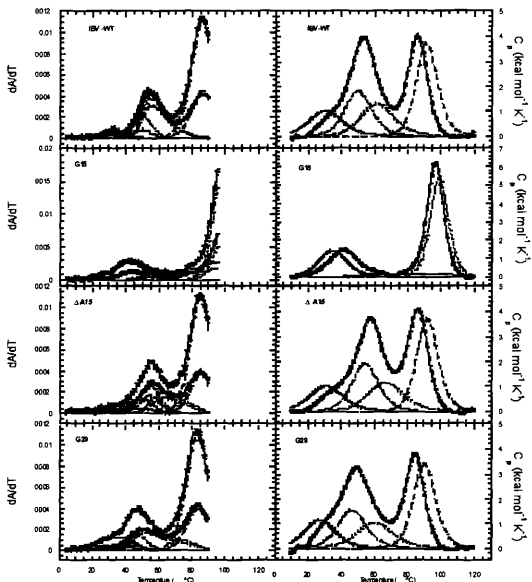


Figure 4. Melts of pseudoknots characterized in Liphardt *et al*, 1999. Melts obtained by optically monitored thermal denaturation are shown on the left. RNA unfolding is monitored at 280 nm (squares) and 260 nm (circles). Melts obtained by DSC are shown on the right. The individual transitions for each melt are displayed as solid or dashed lines below their respective melting profiles.

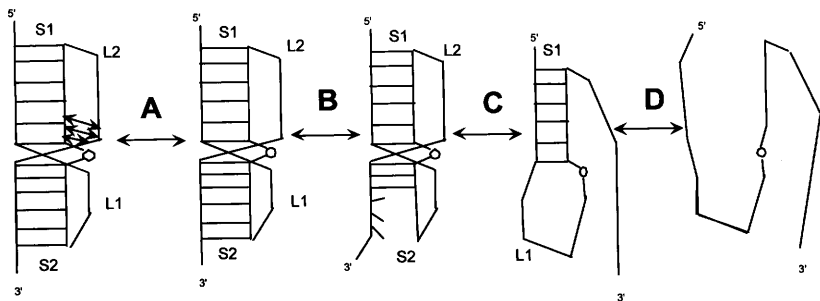


Figure 5. Possible pseudoknot unfolding pathway. The solid lines represent hydrogen bonds, the oval represents an intercalated nucleotide. Transition A represents the collapse of a stem 1 – loop 2 interaction (represented by the arrows in the pseudoknot diagram). Transition B represents the partial unfolding of stem 2, and transition C represents the full unfolding of stem 2 to yield stem 1. It should be pointed out that the unfolding of stem 2 is presented here as a model – it is not known at this time which half of stem 2 unfolds first. Transition D represents the two-state unfolding to stem 1 into fully unfolded RNA.

pseudoknot loop 2 and stem 1 (Figure 5). The second and third unfolding transitions can be modeled below the first high amplitude peak of the melting profile, suggesting that the first helical stem unfolds in a non-two state manner. This means that the stem unfolding pathway goes from a fully folded stem to a partially folded stem, then to a fully unfolded stem (Figure 5). A two state unfolding process would occur when a stem goes from fully folded to fully unfolded. This non-two state behavior is observed in both DSC and optical melts. The final transition has an optical hyperchromicity signature consistent with a stem 1-to-hairpin unfolding transition (Figure 5).

Comparison of the resolved thermodynamic parameters for unfolding of pseudoknots by DSC (Table 1) or optical melts (Table 2) shows a close correlation between the two data sets. Optical data were difficult to fit because of the fact that the instrument can only record absorption data up to 95°C, meaning that a full melting profile of the back slope of the second large transition cannot be accurately measured. This is clearly the case with the G15 RNA melting profile, where the melting temperature occurs near the upper limit of the optical data. This fact may be the origin of some discrepancies between the optical and DSC data for this particular RNA.

Thermodynamic Analysis of the IBV-RNAs

A striking aspect of these results is that the G15 and G29 RNAs, while forming less stable structures than the wild type pseudoknot, both display lowered frameshifting efficiencies. The fact that the removal of the adenosine residue at the stem 1 – stem 2 junction ($\Delta A15$) produces a more stable structure

RNA	Transition	T_m (°C)	ΔH (kcal mol ⁻¹)	$\Delta H_{predicted}$	ΔH_{hot}	ΔH_{cal}	ΔG_{37}^{\ddagger} (kcal mol ⁻¹)	ΔG_{37}^{\ddagger} predicted	ΔG_{37}^{\ddagger} hot	ΔG_{37}^{\ddagger} cal	$\Delta \Delta G_{37}^{\ddagger}$ hot	$\Delta \Delta G_{37}^{\ddagger}$ cal
WT	1	40.3 (0.4)	27.3 (0.7)			0.3 (0.0)						
	2	55.5 (0.4)	38.6 (0.7)			1.8 (0.1)						
	3	59.2 (0.3)	34.0 (1.0)	64.6 (6.5)	67.2 (7.3)	2.3 (0.1)	14.4 (0.4)	15.7 (0.3)	12.9 (0.3)	4.4 (0.2)	0.0 (0.5)	
	4	85.7 (0.1)	62.7 (0.2)	162.8 (2.6)	162.8 (2.6)	8.5 (0.0)	15.7 (0.3)	14.0 (0.2)	14.0 (0.2)	3.4 (0.2)	1.4 (0.5)	
AA15	1	41.1 (0.3)	27.0 (0.4)			0.4 (0.0)						
	2	56.8 (0.2)	40.3 (0.6)			2.4 (0.1)						
	3	64.3 (0.4)	32.5 (0.7)	64.6 (6.5)	67.2 (7.3)	2.6 (0.1)	14.4 (0.4)	15.7 (0.3)	14.0 (0.2)	3.4 (0.2)	1.4 (0.5)	
	4	86.2 (0.0)	62.5 (0.3)	162.3(1.9)	162.3(1.9)	8.6 (0.0)	15.7 (0.3)	14.0 (0.2)	14.0 (0.2)	3.4 (0.2)	1.4 (0.5)	
G15	1	41.5 (0.1)	32.3 (0.4)			0.5 (0.0)						
	2	84.5 (0.5)	12.8 (0.6)			1.7 (0.1)						
	3	95.1 (0.3)	76.9 (0.9)	80.8 (8.5)	122.0 (1.5)	8.8 (0.2)	14.4 (0.4)	19.0 (0.5)	11.0 (0.3)	2.2 (0.3)	-1.9 (0.3)	
	4	84.3 (0.1)	30.2 (1.1)	64.6 (6.5)	67.2 (7.3)	1.3 (0.1)	14.4 (0.4)	15.7 (0.3)	11.1 (0.3)	3.2 (0.2)	-1.4 (0.2)	
G29	1	36.5 (0.4)	28.7 (0.8)			0.0 (0.0)						
	2	49.2 (0.5)	35.5 (0.9)			1.3 (0.1)						
	3	57.8 (0.6)	30.2 (1.1)	64.6 (6.5)	67.2 (7.3)	1.9 (0.1)	14.4 (0.4)	15.7 (0.3)	11.1 (0.3)	3.2 (0.2)	-1.4 (0.2)	
	4	84.3 (0.1)	60.9 (0.3)	64.6 (6.5)	67.2 (7.3)	8.0 (0.1)	14.4 (0.4)	15.7 (0.3)	11.1 (0.3)	3.2 (0.2)	-1.4 (0.2)	

Table 1. Thermodynamic parameters derived from DSC melting profiles of pseudoknots in 10 mM MOPS, 50 mM KCl, pH 7.0. ^aFor WT, AA15, and G29 this value represents the ΔG_{37}^{\ddagger} or $\Delta \Delta G_{37}^{\ddagger}$ value summed for the first unfolding of the three transitions; for G15, this value represents the ΔG_{37}^{\ddagger} or $\Delta \Delta G_{37}^{\ddagger}$ value for the first two transitions. ^bFor purpose of calculating Gibbs free energies for folded pseudoknot relative to the unfolded structures the contribution of proposed G15-C7 base pair in S1 unfolding has been eliminated ($\Delta G = 3.3$ kcal mol⁻¹), since this base pair is not part of the native folded structure and is only formed in the S1 hairpin upon unfolding of the rest of the structure (see text for details).

RNA	Transition	T _m (°C)	ΔH (Kcal mol ⁻¹)	ΔH _{predicted}	ΔG [‡] (Kcal mol ⁻¹)	ΔG [‡] _{predicted}	ΔG [‡] _{rot}	ΔG [‡] _{rot}	ΔΔG [‡] _{rot}	ΔΔG [‡] _{rot}
WT	1	31.5 (0.6)	35.2 (7.2)	64.6 (6.5)	170.3 (10.5)	8.0 (0.3)	14.4 (0.4)	15.7 (0.3)	11.3 (0.4)	3.9 (0.3)
	2	51.8 (0.6)	46.1 (0.4)	64.6 (6.5)	170.3 (10.5)	2.3 (0.3)	14.4 (0.4)	15.7 (0.3)	11.3 (0.4)	0.0 (0.5)
	3	57.5 (1.4)	32.0 (2.8)	64.6 (6.5)	170.3 (10.5)	8.0 (0.3)	14.4 (0.4)	15.7 (0.3)	11.3 (0.4)	3.9 (0.3)
	4	86.6 (0.6)	57.1 (0.1)	64.6 (6.5)	170.3 (10.5)	8.0 (0.3)	14.4 (0.4)	15.7 (0.3)	11.3 (0.4)	3.9 (0.3)
ΔA15	1	41.5 (1.3)	21.7 (3.5)	64.6 (6.5)	159.3 (11.6)	0.3 (0.1)	14.4 (0.4)	15.7 (0.3)	13.6 (1.8)	5.8 (1.2)
	2	55.5 (2.8)	44.9 (1.8)	64.6 (6.5)	159.3 (11.6)	2.5 (0.5)	14.4 (0.4)	15.7 (0.3)	13.6 (1.8)	5.8 (1.2)
	3	65.4 (2.1)	35.4 (4.3)	64.6 (6.5)	159.3 (11.6)	3.0 (0.6)	14.4 (0.4)	15.7 (0.3)	13.6 (1.8)	5.8 (1.2)
	4	85.8 (2.2)	57.2 (2.2)	64.6 (6.5)	159.3 (11.6)	7.8 (0.6)	14.4 (0.4)	15.7 (0.3)	13.6 (1.8)	5.8 (1.2)
G15	1	39.0 (2.1)	32.9 (1.8)	64.6 (6.5)	122.9 (5.8)	0.2 (0.2)	14.4 (0.4)	19.0 (0.5)	10.6 (1.1)	2.3 (0.8)
	2	85.0 (0.0)	15.9 (4.1)	64.6 (6.5)	122.9 (5.8)	2.1 (0.5)	14.4 (0.4)	19.0 (0.5)	10.6 (1.1)	2.3 (0.8)
	3	94.3 (1.7)	74.0 (0.0)	64.6 (6.5)	122.9 (5.8)	8.2 (0.3) ^b	14.4 (0.4)	19.0 (0.5)	10.6 (1.1)	2.3 (0.8)
	4	83.2 (0.8)	54.1 (0.6)	64.6 (6.5)	141.5 (4.0)	-0.3 (0.0)	14.4 (0.4)	15.7 (0.3)	9.3 (0.3)	2.3 (0.1)
G29	1	33.5 (0.8)	22.4 (1.4)	64.6 (6.5)	141.5 (4.0)	-0.3 (0.0)	14.4 (0.4)	15.7 (0.3)	9.3 (0.3)	2.3 (0.1)
	2	46.8 (0.1)	42.2 (1.3)	64.6 (6.5)	141.5 (4.0)	1.3 (0.0)	14.4 (0.4)	15.7 (0.3)	9.3 (0.3)	2.3 (0.1)
	3	57.5 (0.7)	20.8 (0.8)	64.6 (6.5)	141.5 (4.0)	1.3 (0.1)	14.4 (0.4)	15.7 (0.3)	9.3 (0.3)	2.3 (0.1)
	4	83.2 (0.8)	54.1 (0.6)	64.6 (6.5)	141.5 (4.0)	1.3 (0.1)	14.4 (0.4)	15.7 (0.3)	9.3 (0.3)	2.3 (0.1)

Table 2. Thermodynamic parameters from UV melting profiles of pseudoknots in 10 mM MOPS, 50 mM KCl, pH 7.0. For WT, ΔA15, and G29 this value represents the ΔG[‡] or ΔΔG[‡] value for the first three transitions; for G15, this value represents the ΔG[‡] or ΔΔG[‡] value for the first two transitions. ^bFor purpose of calculating Gibbs free energies for folded pseudoknot relative to the unfolded structures the contribution of proposed G15-C7 base pair in S1 unfolding has been eliminated (ΔG = 3.3 kcal mol⁻¹), since this base pair is not part of the native folded structure and is only formed in the S1 hairpin upon unfolding of the rest of the structure (see text for details).

contrasts with previous studies on two other frameshifting RNAs which showed that such a deletion is stabilizing by $\sim 1 \text{ kcal mol}^{-1}$ (Theimer & Giedroc, 1999; 2000). The impact that a deletion or a substitution of the intercalating nucleotide has may be strongly context dependent and not a strong predictor for pseudoknot stability.

The G15 mutant RNA displays a distinct optical melting profile. Data collected from the DSC melt (shown in Table 1) reveals that the first stem unfolding transition occurs at a far lower temperature (41.5°C for G15, approximately 50°C for the other pseudoknots), with considerable less ΔH associated with this unfolding transition. The second stem unfolding of the second stem, stem 1, on the other hand, occurs at a higher temperature (almost 10°C higher) with a comparably larger enthalpy of unfolding (approximately 10 kcal mol^{-1} greater). This finding is most easily explained by the fact that the guanosine 15 of this structure could form a Watson-Crick base pair with cytosine 7, the first residue of loop 1, upon deconstruction of the pseudoknot fold. This would result in the formation of a seven base pair stem 1 hairpin, predicted to induce a $13.4 \text{ kcal mol}^{-1}$ increase in ΔH_{tot} , and an increase in increase in ΔG^{37} of $3.3 \text{ kcal mol}^{-1}$ (Xia *et al.*, 1998). The thermodynamic parameters for the unfolding of the stem 1 hairpin in the G15 RNA is in close approximation to these predicted values.

Substitution of the adenosine 29 nucleotide in loop 2 with guanosine brings about the formation of a destabilized pseudoknot structure. A comparison with the wild type structure shows that unfolding transitions of G29 occurs with

smaller enthalpies at lowered t_m values. It was originally postulated that this nucleotide was important in stabilizing an interaction with stem 1. The thermodynamic data reported here are consistent with that scenario, with these interactions contributing $\sim 1.5 \text{ kcal mol}^{-1}$ in global stability to the pseudoknot. Our research group has had similar findings in the beet western yellows virus pseudoknot (S. Suram and D.P. Giedroc, unpublished results). NMR structural studies of the wild-type IBV-MMTV chimeric RNA should provide structural insight into this stabilization.

ΔG_{tot} vs. Frameshifting Efficiency

Given the t_m values and van't Hoff enthalpies for each transition, the Gibbs free energy can be calculated for each unfolding transition, which are then summed to determine ΔG_{tot} for each pseudoknot. From this, values of $\Delta\Delta G_{\text{tot}}^{37}$ ($\Delta\Delta G_{\text{mutant}}^{37} - \Delta\Delta G_{\text{wild type}}^{37}$) values are calculated. However, a better way to compare the thermodynamic parameters in each of these mutations is to calculate the stability of the folded pseudoknotted structure relative to the partially folded stem 1 hairpin. This stability value is given by $\Delta G_1 + \Delta G_2 + \Delta G_3 = \Sigma\Delta G_{1-3}$. Comparison with wild-type RNA gives $\Delta\Delta G_{1-3}^{37}$. A plot showing the relationship between frameshifting efficiency and $\Delta\Delta G_{1-3}^{37}$ is shown in Figure 6. This plot suggests no clear relationship between stability and frameshifting efficiency. The mutant pseudoknot with the highest frameshifting efficiency (G15 – 12%) formed a structure approximately as destabilized as the mutant pseudoknot with the lowest frameshifting efficiency (G29 – 5%). The $\Delta A15$

pseudoknot, despite having a structure stabilized relative to WT, is still an inefficiently frameshifting construct.

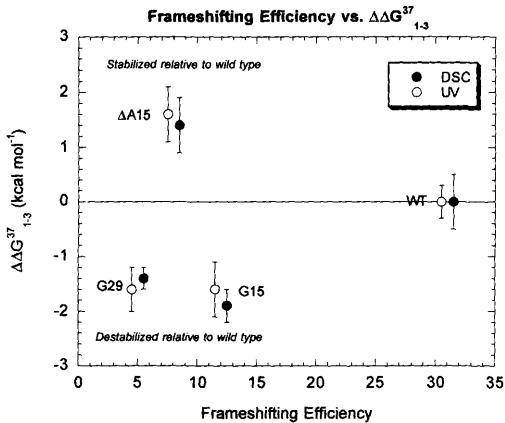


Figure 6. Plot of frameshifting efficiency vs. $\Delta\Delta G_{1-3}^{37}$ values obtained from UV and DSC data.

CHAPTER 3

CONCLUSIONS

In a recent review, three models were suggested by which pseudoknots could stimulate ribosomal frameshifting (Giedroc *et al*, 2000). The first model is that frameshifting efficiency is influenced by some specific aspect of the pseudoknot structure, which could mediate an interaction with some part of the ribosome. The second model suggests that there is some free energy difference between folded and partially folded states of the pseudoknot that gives rise to frameshifting. The third model suggests that frameshifting efficiency is dictated at the level of kinetics, where local energetics dictate the *rate* at which the pseudoknot is resolved to the stem 1 hairpin.

The findings of this report are brought to bear on the second model, in which the -1 frameshifting process is addressed at the level of the thermodynamic stability of the RNA pseudoknot. Our studies suggest that there is not a strong correlation between thermodynamic stability of RNA pseudoknots and frameshifting stability in the context of the four pseudoknots studied here. Despite this lack of a strong correlation between frameshifting efficiency and pseudoknot stability, insight into the energetic penalties which result from deletions or substitutions of two key structural elements, the intercalated adenosine and 3' nucleotide of loop 2, have been quantified. Detailed structural studies which pinpoint the origin of these thermodynamic perturbations will be of high interest. This suggests that future studies which seek to understand the

mechanism of frameshifting will most likely address either the detailed structure or the kinetics of unwinding of RNA pseudoknots.

CHAPTER 4

MATERIALS AND METHODS

RNA Purification

RNA was transcribed using partially double stranded DNA containing a T7 promoter region. Large scale transcription reactions were run for 4_ hours at 37°C, and ethanol precipitated. The RNA was then run over a G25 sephadex column, and purified on a denaturing PAGE gel. Bands were detected using UV monitoring, and electroeluted for 9 hours. RNA was then cartridge filtered, and eluted with a 50% methanol solution. It was then dried, resuspended in water, and exhaustively dialyzed in 10 mM MOPS, 50 mM KCl for 9 hours, with dialysis buffer changed every 3 hours. The first dialysis was made approximately 2 mM in EDTA.

UV Thermal Denaturation

All samples analyzed by optically monitored thermal denaturation consisted of 600 μ l of 3 μ M RNA in a buffer of 10 mM MOPS and 50 mM KCl, plus the indicated concentration of Mg^{2+} . Samples were subjected to thermal denaturation using a Cary 1 UV / Vis spectrophotometer operating in double beam mode. Percentage transmittance, collected as a function of temperature at the rate of 0.3 degrees per minute, was converted to absorbance and the first derivative with respect to temperature was fit to a multiple sequential interacting transition model, as has been described previously (Nixon and Giedroc, 1998; Theimer *et al*, 1998; Theimer & Giedroc, 1999).

Differential Scanning Calorimetry Denaturation

DSC traces were obtained using a Microcal VP-Differential Scanning Calorimeter. Samples were prepared by diluting stock solutions of RNA to a 1 ml solution of $>40 \mu\text{M}$, and then dialyzing for 10 hours in a 10 mM MOPS, 50 mM KCl buffer. Following denaturation, the final concentration was determined by adding $40 \mu\text{l}$ of 2 M KOH to diluted calorimetry samples. The addition of base was performed to correct for the hyperchromic effect. Samples were corrected for dilution and A_{260} measurements were used to determine the exact concentration of each calorimetry sample.

DSC reference scans were subtracted from DSC samples scans to give reference subtracted data. This curve (C_p vs. Temperature) was normalized to the exact concentration of sample RNA, and subjected to a linear baseline approximation method and fit to an appropriate number of sequential interacting transitions to calculate $\Delta H_{vH,i}$ and $t_{m,i}$. The area under the normalized curve was calculated to give the total enthalpy of denaturation, ΔH_{cal} . DSC analysis was accomplished using Origin DSC software from Microcal Inc.

REFERENCES

- Brierly, I., Digard, P. & Inglis, S.C. (1989). Characterization of an efficient cononavirurs ribosomal frameshifting signal: requirement for an RNA pseudoknot. *Cell*, **57**, 537-547.
- Farabaugh, P.J. (1993). Programmed translational frameshifting. *Microbiol. Rev.* **60**, 103-134.
- Giedroc, D.P., Theimer, C.A., Nixon, P.L. (2000). Structure, Stability and Function of RNA Pseudoknots Involved in Stimulating Ribosomal Frameshifting. *J. Mol. Biol.* **298**, 167-185.
- Kolk, M.H., van der Graaf, M., Wijmenga, S.S., Pleij, C.W.A., Heus, H.A. & Hilbers, C.W. (1998). NMR structure of a classical pseudoknot: interplay of single- and double-stranded RNA. *Science*, **280**, 434-438.
- Liphardt, J., Napthine, S., Kontos, H. & Brierly, I. (1999). Evidence for an RNA pseudoknot loop-helix interaction essential for efficient -1 ribosomal frameshifting. *J. Mol. Biol.* **288**, 321-335.
- Napthine, S., Liphardt, J., Bloys, A., Routledge, S., & Brierly, I. (1999). The Role of RNA Pseudoknot Stem 1 Length in the Promotion of Efficient -1 Ribosomal Frameshifting. *J. Mol. Biol.* **288**, 305-320.
- Nixon, P.L., & Giedroc, D.P. (1998). Equilibrium unfolding (folding) pathway of a model H-type pseudoknotted RNA: the role of magnesium ions in stability. *Biochemistry*. **37**, 305-320.
- Pleij, C.W.A. (1990). RNA Pseudoknots. *Curr. Opin. in Stru. Biol.* **4**, 337-344.
- Shen, L.X., & Tinoco, I. (1995). The structure of an RNA pseudoknot that causes efficient frameshifting in mouse mammary tumor virus. *J. Mol. Biol.* **247**, 963-978.
- Su, L., Chen, L., Egli, M., Berger, J.M. & Rich, A. (1999). Minor groove RNA triplex in the crystal structure of a ribosomal frameshifting viral pseudoknot. *Nature Struct. Biol.* **6**, 285-292.
- Theimer, C.A., Giedroc, D.P. (1999). Equilibrium unfolding pathway of an H-type RNA pseudoknot which promotes programmed -1 ribosomal frameshifting. *J. Mol. Biol.* **289**, 1283-1299.

- Theimer, C.A., Giedroc, D.P. (2000). Contribution of the intercalated adenosine at the helical junction to the stability of the *gag-pro* frameshifting pseudoknot from mouse mammary tumor virus. *RNA*. **6**. 409-421.
- Theimer, C.A., Wang, Y., Hoffman, D.W., Krisch, H.M., Giedroc, D.P. (1998). Non-nearest neighbor effects on the thermodynamics of unfolding of a model mRNA pseudoknot. *J. Mol. Biol.* **279**. 545-564.
- Xia, T., SantaLucia, J., Jr., Burkard, M.E., Kierzek, R., Shroeder, S.J., Jiao, X., Cox, C. & Turner, D.H. (1998). Thermodynamic parameters for an expanded nearest-neighbor model for formation of RNA duplexes with Watson-Crick base-pairs. *Biochemistry*. **17**. 14719-14735.

VITA**BRIAN RAY CANNON****Personal Information:**

Birthdate: February 4, 1979

Address: 19 Robin Run
The Woodlands, TX 77844

Electronic mail address: brian_ray_cannon@hotmail.com

Educational Background:

1995-1997 The Woodlands High School
The Woodlands, TX

1997-2001 B.S., Biochemistry
Texas A&M University
College Station, TX

Honors:

1997-2001 Texas A&M Academic Scholarship

1997-2001 HHMI Undergraduate Research Fellow

Experience:

1997 Summer Undergraduate Research Fellowship
Baylor University
Waco, Texas

1998 Summer Undergraduate Research Program
UT Southwestern
Dallas, Texas